

# How to Implement Mutual Network Synchronization in the Presence of Large Cross-Coupling Delays

L. Wetzel, D. Prousalis, F. Jülicher

Max Planck Institute for the Physics of Complex Systems  
Dresden, Germany  
lwetzel@pks.mpg.de

R. Riaz, C. Hoyer, N. Joram, F. Ellinger

Chair for Circuit Design and Network Theory,  
Technische Universität Dresden, Germany  
niko.joram@tu-dresden.de

**Summary**—*Mutual synchronization without a reference oscillator has shown to scale advantageously with system size while being robust to noise. However, the complexity of its implementation has so far hindered its way into technical application. We show that the issue can be addressed using concepts from delay dynamical systems theory. These allow to predict the properties of self-organized synchronization, necessary to guide the architecture design of networks that implement the mutual synchronization concept. We confirm the theoretical predictions with numerical simulations.*

**Keywords**—*network synchronization, control theory*

## I. INTRODUCTION

Synchronization orchestrates complex distributed systems in time, ranging from biology to engineering [1]–[5]. In engineering the hierarchical approach to synchronization has become dominant – a high quality reference oscillator entrains distributed electronic oscillators such as phase-locked loops (PLL) [5]. In biology the orchestration of processes in time is usually found to be non-hierarchical [2]. It relies on the mutual interactions of oscillators or periodic processes and is termed mutual synchronization.

The distribution of clocking signals with constant phase differences in complex spatially distributed systems provides a precise common time reference [6]. Ideally, the phase differences are zero. This is, e.g., relevant in data centers, mobile communications, navigation and localization applications. In the presence of unavoidable cross-coupling time delays this can be achieved particularly well with the mutual synchronization approach [7,8]. Contrary to hierarchical synchronization concepts, such time delays do not induce phase differences in networks of mutually coupled oscillators. Furthermore, mutual synchronization scales advantageously with system size and is robust to noise. Its implementation however, is a complex task [4] and the theoretical basis had so far not been well established. Even though it is suited to serve the requirements of clocking signal distribution in modern spatially distributed systems that operate at high frequencies, it is currently not widely used [9].

In this work we show in Sec. II how the complexity of the implementation of mutual synchronization can be addressed using tools from delay dynamical systems theory. These can predict the properties of synchronized states and their stability in networks of mutually delay-coupled oscillators. Using them

allows to analyze how the free parameters in such networks need to be tuned to achieve stable synchronization in the presence of, e.g., large cross-coupling time delays. In Sec. III we present simulation results for large networks and time delays. They confirm that using the theoretical results the architecture design for such synchronization layers can be informed, see discussion and conclusions in Sec. IV.

## II. THE PROPERTIES OF SYNCHRONIZED STATES

For a network of  $N$  coupled PLLs one finds for the dynamics of the PLLs' instantaneous frequencies [10]

$$\dot{\phi}_k(t) = \omega_k + \frac{K_k}{n(k)} \sum_{l=0}^{N-1} c_{kl} \int_0^\infty du p_k(u) h\left(\frac{\phi_l(t-u-\tau_{kl}) - \phi_k(t-u)}{v}\right), \quad (1)$$

where  $k = 1, \dots, N$  indexes the  $N$  PLLs in the network,  $\omega_k$  denotes the intrinsic angular frequency of PLL  $k$ ,  $K_k$  the coupling strength, which contains all the gains of the feed forward path,  $n(k)$  the number of input signals,  $c_{kl}$  the components of the network's adjacency matrix being either one if there is a connection from PLL  $l$  to  $k$  or zero otherwise,  $p_k(u)$  the impulse response function of the loop filter,  $\tau_{kl}$  the cross-coupling time delay from node  $l$  to  $k$ , and  $v$  the divisor of the frequency divider. The coupling function  $h(\cdot)$  is a  $2\pi$ -periodic function of the phase differences between the feedback and input signals. For digital PLLs the coupling function then is triangular (XOR phase detector), for analog PLLs sinusoidal (multiplier). The ansatz for globally phase-locked states is  $\theta_k(t) = \Omega t + \beta_k$ , where  $\Omega$  denotes the global frequency and  $\beta_k$  the phase offset with respect to the choice  $\beta_0 = 0$ .

**Frequency and phase relations:** In [4], the global frequency of in-phase synchronized states was calculated after linearizing the coupling function  $h(\cdot)$

$$\Omega = \frac{\frac{\omega_k v}{K_k}}{\frac{v}{K_k} + \frac{1}{n(k)} \sum_l c_{kl} \tau_{kl}}. \quad (2)$$

This expression shows, see Fig.1, that the frequency of the synchronized state is decreasing as the delay is increased. Hence, phenomena, such as e.g., the multistability, which have been found in experiments [10], were not studied in [4]. In

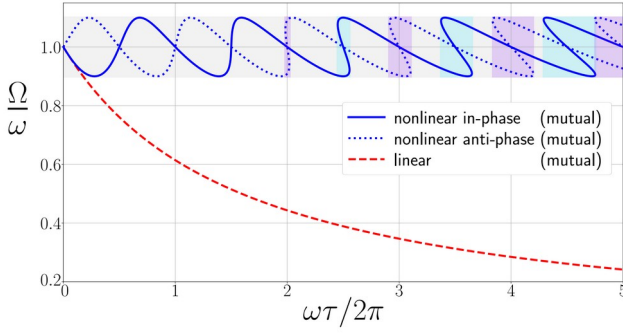


Fig. 1: Frequencies of synchronized states vs the cross-coupling time delay using the linearized model (red) and using the nonlinear model (blue) for a system of  $N=2$  coupled identical oscillators with sinusoidal coupling function  $h(\cdot)$ . PLL parameters are  $\omega = 2\pi \cdot 24$  GHz,  $K = 2\pi \cdot 2.4$  GHz/V,  $v=1$ . We show in gray the multistability of in- and anti-phase states. In cyan and purple the multistability within in- and anti-phase synchronized states, respectively.

contrast, such phenomena can be studied and analyzed using the non-linear expression of the model Eq. (1). Given the nonlinear coupling, the frequencies of synchronized states are

$$\Omega = \omega_k + \frac{K_k}{n(k)} \sum_{l=0}^{N-1} c_{kl} h\left(\frac{-\Omega\tau_{kl} - \beta_{kl}}{v}\right), \quad (3)$$

where  $\beta_{kl} = \beta_k - \beta_l$ . Eq. (3) is implicit in  $\Omega$ , and hence multistability of synchronized states with different frequencies can occur for the same set of system parameters, see Fig. 1. For identical oscillators, Eq. (3) is independent of the number of oscillators and  $\beta/v = \beta_{kl}/v \in \{0, \pi\}$ . In Fig. 1, we compare the frequencies obtained from Eq. (2) and Eq. (3) as a function of the cross-coupling time delay  $\tau$  [11]. We plot solutions to Eq. (3), namely in- ( $\beta = 0$ ) and anti-phase ( $\beta = \pi$ ) synchronized states that coexist in such a network [10]. Comparison shows that the linearized model is valid for small cross-coupling time delays.

**Linear stability of synchronized states:** The stability of self-organized synchronous states can be studied using concepts from delayed dynamical systems theory [11]. We discuss, how taking into account the nonlinear coupling, the nodes' steady state loop gains, their phase and gain margins and those of the network become state-dependent [11]. Using these, the linear stability of self-organized synchronous states can be predicted using the so called characteristic equation. For identical oscillators and first order RC loop filters it can be shown that the characteristic equation has the following form [12]

$$\lambda^2 + \omega_c \lambda + \alpha \omega_c (1 - \zeta e^{-\lambda\tau}), \quad (4)$$

where  $\lambda = \sigma + i\gamma$  is the Laplace variable whose real part  $\sigma$  informs whether small perturbations to a synchronized state grow ( $\sigma > 0$ , unstable state) or decay ( $\sigma < 0$ , stable state). The imaginary part  $\gamma$  denotes the frequency associated to the perturbation response, i.e.,  $\gamma \neq 0$  implies that perturbation decay is underdamped and  $\gamma = 0$  that it is overdamped. The

parameter  $\alpha = \frac{K}{v} h'\left(\frac{-\Omega\tau - \beta}{v}\right)$  depends on the properties of the synchronized states and denotes the feed-forward steady state loop gain of the PLLs,  $\tau$  denotes the transmission time delay in the coupling and  $\omega_c$  the angular cut-off frequency of the loop filter.

In the case of heterogeneous oscillators the characteristic equation can be obtained from solving  $\det(\mathbb{G} - \mathbb{I})$ , where  $\mathbb{I}$  denotes the identity matrix and  $\mathbb{G}$  has entries  $G_{kl}$  for each connection between an oscillators  $k$  and  $l$  in the network [13]

$$G_{kl} = \tilde{c}_{kl} \alpha_{kl} e^{-\lambda\tau_{kl}} \left( \frac{\lambda}{\hat{p}_k(\lambda)} + \sum_{l'=1}^N \tilde{c}_{kl'} \alpha_{kl'} \right)^{-1}. \quad (5)$$

The  $\tilde{c}_{kl}$  are equal to either  $1/n_k$  or 0 and denote whether there is a connection from oscillator  $k$  to  $l$  or not respectively,  $n_k$  denotes the number of inputs to oscillator  $k$ ,  $\alpha_{kl}$  denotes the feed-forward path loop gain of an oscillator  $k$  in the network with respect to its input from another oscillator  $l$  in the network,  $\tau_{kl}$  the transmission time delay from oscillator  $k$  to  $l$ , and  $\hat{p}_k(u)$  the impulse response function of the loop filter. Note, that the  $G_{kl}$  are connected to the individual transfer function  $H_{kl}^{\text{FF}} = \alpha_{kl} \hat{p}_k(\lambda)/\lambda$  of a feed-forward path from input  $l$  of PLL  $k$ . With this identification one can show that for identical cross-coupling time delays and PLL parameters the properties of the network decouple from those of the PLLs [11]. Heterogeneous oscillator networks are discussed in [13].

In [12] it has been shown how the exponential polynomial in Eq. (4) can be analyzed to obtain criteria and a sufficient condition for the stability of in- and anti-phase synchronized states in networks of identical oscillators. These criteria and the condition are used here to obtain a parameter space plot

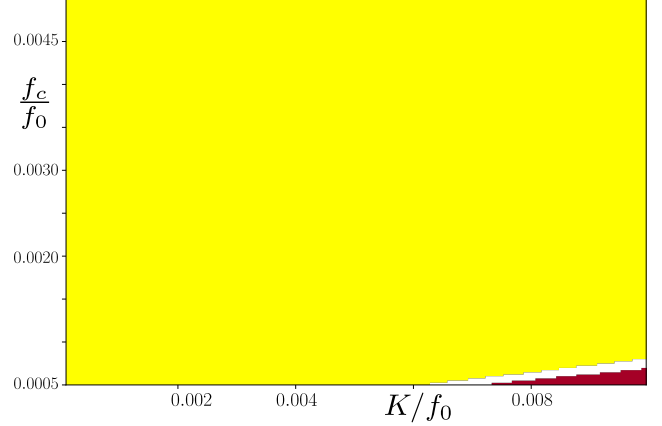


Fig. 2:  $f_c$ - $K$  parameter space plot for  $N = 256$  PLLs on a  $2d$   $16 \times 16$  square grid with open boundary conditions and nearest neighbor interactions. The cross-coupling time delay equals 1003.52 multiples of the period of the intrinsic period of the PLLs and the frequency division is  $v = 16$ . Both axes are normalized by  $f_0 = 125$  MHz the intrinsic frequency of the oscillators. The colors denote the stability of synchronized states. In the white and yellow colored regimes, in-phase synchronized states are predicted to be linearly stable, while in the red regimes they are unstable. The stability in the white regime cannot be understood from the sufficient stability condition but requires applying the criteria presented in [11].

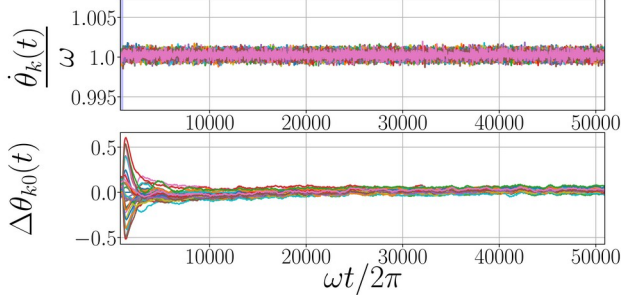


Fig. 3: Time-series of frequencies and phase-differences for  $N = 256$  mutually delay-coupled heterogeneous PLLs with intrinsic frequency  $f_0 = 125$  MHz arranged on a 2-dimensional  $16 \times 16$  square grid with open boundary conditions and nearest neighbor interactions. The mean loop filter cut-off frequency of the PLLs is  $\bar{f}_c = 156.25$  kHz and the mean coupling strength is  $\bar{K} = 625$  kHz. For the simulation, the values of the cut-off frequencies and coupling strengths are identically distributed in the intervals  $[125, 187.5]$  kHz and  $[623.75, 626.25]$  kHz, respectively. The frequency of the cross-coupling signals is the frequency of the output signals divided by 16.

of the loop filter cut-off frequency vs. the coupling strength of the oscillators for a fixed value of the time delay and the frequency division, see Fig. 2. Hence, in a situation where oscillators need to be synchronized at a predetermined distance, i.e., the transmission time delays between them is fixed to a certain regime, such parameter space plots help to tune the properties of the oscillators such that stable synchronized states can be achieved. This is shown in the next section in numerical simulations of a network of mutually coupled PLLs in the presence of considerable transmission time delay.

### III. NUMERICAL SIMULATION

The simulations presented in this section are carried out using an Euler scheme for Eq. (1) with the time increment being equal to  $dt = 1/(55 f_0)$ . Hence, the resulting signals are sampled with 55 points per period of the free-running oscillators. Note, that for first order loop filters the delay integro-differential Eq. (1) can be expressed as a set of two coupled first order differential equations. One of these represents the time evolution of the control signal that controls the PLLs voltage controlled oscillator (VCO), while the other represents the time evolution of the instantaneous frequency of the PLL output signal. As an example we present a network of  $N = 256$  mutually delay-coupled PLLs with noisy VCO output, arranged on a 2-dimensional square grid with nearest neighbor coupling and open boundary conditions. Assume the cross-coupling delays are set to be equivalent to 1003.52 times the intrinsic periods of the PLLs by the application, i.e., related to node to node distances of about 2400 meters. The oscillators have an intrinsic frequency  $f_0 = 125$  MHz, a mean loop filter cut-off frequency of  $\bar{f}_c = 156.25$  kHz (1<sup>st</sup> order RC), and are cross-coupled at a frequency division of  $v = 16$ . Then, using the theoretical tools we can predict for which PLL coupling strength there is a

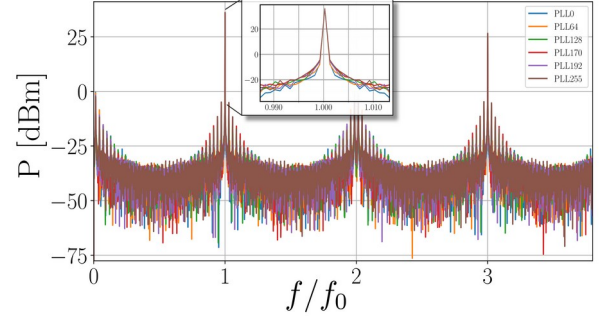


Fig. 4: Power spectral densities of the digital signals of the phases – computed using  $4.2 \mu s$  of the time series and a boxcar window function. The frequency resolution is  $\Delta f \approx 125$  kHz, the sampling frequency  $f_s = 6.875$  GHz. Here, only the oscillators indexed by  $k = \{0, 64, 128, 170, 192, 255\}$  are plotted. The inset is a zoom of the principal peak at  $f = \Omega/2\pi$  and suggests that the perturbation decay dynamics are overdamped.

linearly stable synchronized state. Here we choose a loop gain of  $\alpha = 24.9$  kHz/V and compute that the perturbation response is overdamped and hence we expect no characteristic shoulders at  $\Omega \pm \gamma$  in the PSD. The time series of the frequencies and phase-differences are shown in Fig. 3. The initial phases of the oscillators were identically distributed in the range  $[-\pi/25, \pi/25]$  and the oscillators were running uncoupled with each other for  $t \in (-\tau, 0]$ . At  $t = 0$  the mutual coupling between the oscillators is activated. The power spectral density in Fig. 4 is obtained by extracting an integer number of periods of the asymptotic output signal and using a boxcar windowing function. As predicted by the numerically obtained perturbation response rate and frequency the in-phase synchronized state is stable and there are no shoulders associated to underdamped perturbation decay visible close to the principal peak. That the perturbation response is overdamped can also be seen in Fig. 3. The last plot we show for this system is Fig. 5, it shows the time evolution of Kuramoto order parameter of the system. The Kuramoto order parameter quantifies the coherence of the oscillators and is defined as

$$R(t) e^{j\Psi(t)} = \frac{1}{N} \sum_{l=0}^{N-1} e^{j\theta_l(t)}, \quad (6)$$

where  $\Psi(t)$  denotes the phase of the mean field and  $R(t)$  the magnitude of the order parameter.  $R(t) = 1$  if the phases of all oscillators are equal and  $R(t) = 0$  if the phases are equally distributed in  $[0, 2\pi)$ . Fig. 5 shows how the order parameter increases from its initial value and approaches one after about 4000 cycles.

As an example for underdamped perturbation decay we present simulation results for a network of  $N = 64$  mutually delay-coupled PLLs with noisy VCO output, arranged on a 2d square grid with nearest neighbor coupling and open boundary conditions. The cross-coupling delays are set to be equivalent to 39968 times of the intrinsic periods of the PLLs as given by

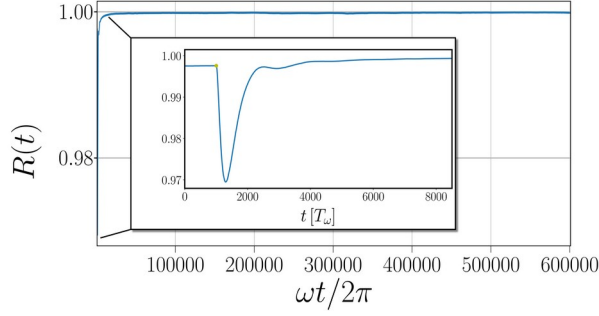


Fig. 5: Kuramoto order parameter for the time evolution of the system as shown in Fig. 3. It approaches one asymptotically and we conclude that the system is in an in-phase synchronized state. The inset shows the transients at the start of the simulation.

an application, i.e., related to node to node distances of about 500 meters. The oscillators intrinsic frequency is  $f_0 = 24$  GHz. The PLLs have a 2<sup>nd</sup> order RC loop filter (implemented via two 1<sup>st</sup> order RC elements in series and a buffer) cut-off frequency  $f_c = 2.4$  MHz and are cross-coupled at a frequency division of  $v = 512$ . Then, using the theoretical tools we can predict for which PLL node gains there is a linearly stable synced state. We predict shoulders in the PSD at  $\Omega \pm \gamma$ , where  $\gamma/\omega = 3.48 \cdot 10^{-5}$ . A time-series simulation of the dynamics of this network then validates the predictions [14]. We find  $\Delta f/f_\omega \approx 4 \cdot 10^{-5}$  from the Fourier analysis of the periodic signals' time-series, see Fig. 6. The prediction is made for the deterministic case without dynamical oscillator noise which can explain the deviation of  $\gamma$  from the simulation results. The data based on which Fig. 6 has been made has been shown before in [11].

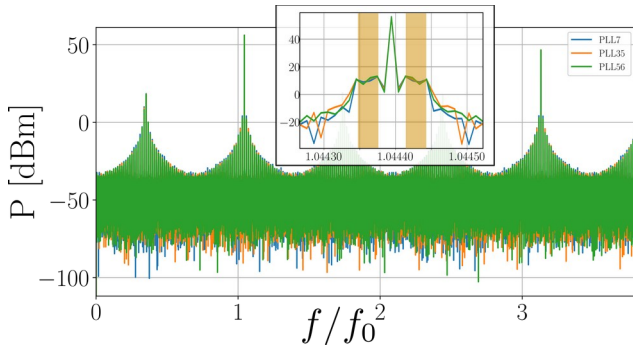


Fig. 6: Power spectral densities of the digital signals of the phases – computed using  $t = 4.2 \mu s$  of the time series and a boxcar window function. The frequency resolution is  $\Delta f \approx 240$  kHz, the sampling frequency  $f_s = 1.32$  THz. Here, only the oscillators indexed by  $k = \{7, 35, 56\}$  on a  $8 \times 8$  2d square grid with nearest neighbor interactions and open boundary conditions are plotted. The inset is a zoom of the principal peak at  $f = \Omega/2\pi$  and suggests that the perturbation decay dynamics are overdamped.

#### IV. DISCUSSION & CONCLUSIONS

Mutual network synchronization can lead to precise phase synchronization in spatially distributed systems, e.g., required for high precision localization, smart grids, ad-hoc network structures, sensor arrays, distributed experimental devices, radar applications and distributed massive MIMO. This

precision is achieved with mutual synchronization since in-phase synchronized states with zero phase differences can be stable even at large cross-coupling time delays. In this work we show how stable synchronization in the presence of large cross-coupling time delays can be achieved. In a first step we use theoretical models that take into account the nonlinear coupling function. We analyze how the free parameters of the oscillator network need to be tuned to achieve stable synchronization given the fixed parameters, e.g., the cross-coupling time delays. This theoretical framework predicts the whether perturbations to a synchronized state decay or grow. For stable synchronized states the framework also predicts whether the perturbation decay is under- or overdamped. Hence, the complex dynamics in such networks can be analyzed. With this work, we address the complexity of the implementation of mutual network synchronization. In numerical simulations we confirm the theoretical predictions for large networks of mutually delay-coupled oscillators.

#### REFERENCES

- [1] A. Pikovsky, M. G. Rosenblum, and J. Kurths, *Synchronization, A Universal Concept in Nonlinear Sciences*. Cambridge University Press, 2001.
- [2] A. C. Oates, L. G. Morelli, and S. Ares, “Patterning embryos with oscillations: structure, function and dynamics of the vertebrate segmentation clock,” *Development*, vol. 139, no. 4, pp. 625–639, 2012.
- [3] V. Flunkert, S. Yanchuk, T. Dahms, and E. Schöll, “Synchronizing Distant Nodes: A Universal Classification of Networks,” *Phys. Rev. Lett.*, vol. 105, p. 254101, 2010.
- [4] W. C. Lindsey, F. Ghazvinian, W. C. Hagmann, and K. Dessouky, “Network synchronization,” *Proc. IEEE*, vol. 73, no. 10, pp. 1445–1467, 1985.
- [5] R. Best, *Phase-Locked Loops*, ser. Professional Engineering. McGraw-Hill, 2003.
- [6] A. Gersho and B. J. Karafin, “Mutual synchronization of geographically separated oscillators,” *Bell Syst. Tech. J.*, vol. 45, no. 10, pp. 1689–1704, 1966.
- [7] K. O’Keefe, H. Hong, and S. Strogatz, “Oscillators that sync and swarm,” *Nat. Commun.*, vol. 8, p. 1504, 2017.
- [8] M. S. Innocente and P. Grasso, “Self-organising swarms of firefighting drones: Harnessing the power of collective intelligence in decentralised multi-robot systems,” *J. Comput. Sci.*, vol. 34, pp. 80–101, 2019.
- [9] C. Hoyer, D. Prousalis, L. Wetzel, R. Riaz, J. Wagner, F. Jülicher, F. Ellinger, “Mutual Synchronization with 24 GHz Oscillators,” *IEEE Int. Symp. Circuits Syst.*, pp. 1–5, 2021.
- [10] L. Wetzel, D. J. Jörg, A. Pollakis, W. Rave, G. Fettweis, and F. Jülicher, “Self-organized synchronization of digital phase-locked loops with delayed coupling in theory and experiment,” *PLOS ONE*, vol. 12, no. 2, pp. 1–21, 2017.
- [11] L. Wetzel, D. Prousalis, R. Riaz, C. Hoyer, N. Joram, J. Fritzsche, F. Ellinger, and F. Jülicher, “Network Synchronization Revisited: Time Delays in Mutually Coupled Oscillators,” 2021 (submitted to *IEEE Access*).
- [12] D. Prousalis, L. Wetzel, “Synchronization in the presence of time delays and inertia: Stability criteria,” *Phys. Rev. E*, vol. 105, p. 014210, 2022.
- [13] N. Punetha and L. Wetzel, “How clock heterogeneity affects synchronization and can enhance stability,” (accepted *Phys. Rev. E*)
- [14] L. Wetzel, D. Platz and A. Pollakis, Github repository available at [github.com/cuichi23/sim\\_pll\\_networks](https://github.com/cuichi23/sim_pll_networks).